JOURNAL OF APPLIED ELECTROCHEMISTRY 22 (1993) 1310–1316

A model of the electrochemical behaviour within a stress corrosion crack

DELIN LI

Department of Mechanical Engineering, Vanderbilt University, Nashville, TN37235, USA

Z. HUANG

Department of Materials Science and Engineering, Beijing University of Aeronautics & Astronautics, People's Republic of China

Received 19 December 1991; revised 15 May 1993

A mathematical model of the electrochemical behaviour within a stress corrosion crack is proposed. Polarization field, crack geometry, surface condition inside the crack, electrochemical kinetics, solution properties and applied stress can be represented by the polarization potential and current, the electrochemical reactive equivalent resistance of the electrode, the change in electrolyte specific resistance and surface film equivalent resistance, respectively. The theoretical calculated results show that (i) when anodic polarization potential is applied, the change in the crack tip potential is small; (ii) when cathodic polarization potential is applied, the crack tip potential changes greatly with the applied potential; (iii) the longer the crack, the smaller the effect of the applied potential on the crack tip potential in both anodic polarization and cathodic polarization conditions. The calculated results are in good agreement with previous experimental results.

Notation

x	coordinate, from crack mouth (on the metal surface) to crack tip (cm)
y	$y = s_L L/(s_0 - s_L) + L - x$, function of x (cm)
y_0	$y_0 = s_L L/(s_0 - s_L) + L$ (cm)
V	polarization potential (V)
φ_x	galvanic potential of electrode (V)
φ_l	galvanic potential of electrolyte (V)
t	sample thickness (cm)
w	sample width (cm)
s_L	crack tip width (cm)
S_o	crack mouth width (cm)
L	crack length (cm)
$s(x)$	crack width at position x (cm)
ρ_{lo}	specific resistance of electrolyte, as a constant (Ω cm)
ρ_s	specific resistance of metal (Ω cm)
$\rho_l(\eta, y)$	specific resistance of electrolyte, varies with potential and crack depth (Ω cm)
$R_b(\eta, y)$	electrochemical reactive equivalent resistance of electrode, varies with potential and crack depth (Ω)
R_l	electrolyte resistance (Ω)
R_s	metal resistance (Ω)
$r(\eta, y)$	surface film equivalent resistance, varies with potential and crack depth (Ω)
r_o	surface film equivalent resistance, as a constant (Ω)
I_o	total polarization current (A)
I	net polarization current from integrating 0 to x in Fig. 2 (A)
η	polarization overpotential (V)
η_a	anodic polarization overpotential (V)
η_c	cathodic polarization overpotential (V)
Υ	Euler's constant

1. Introduction

The electrochemical behaviour within a stress corrosion crack is of great importance in governing the rate of crack propagation in stress corrosion cracking. Doig and Flewitt [1–3] have considered the variation of potential along a stress corrosion crack. The use of the special boundary condition made the integration simple. These conditions are valid only for a semi-infinite crack. Doig and Flewitt's analysis was extended to examine the effect of an arbitrary relation between the current and the potential at a crack tip, and to obtain an analytic solution for those conditions where the variation in potential was small. Melville [4, 5] has studied the variation of potential within a stress corrosion crack with different boundary conditions. The crack was assumed to be either of constant width or to have a linear variation of the crack width between the crack tip and the mouth. The investigations above either obtained the theoretical equations or reported the theoretical analysis. A significant limitation in previous studies is the lack of a

0021-891X

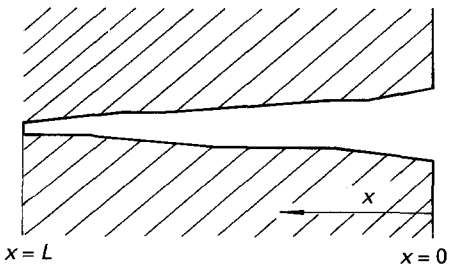

Fig. 1. A schematic illustration of a stress corrosion crack.

quantitative calculation. Obviously, the theoretical calculation is of great importance for understanding the stress corrosion cracking processes.

In this paper, we focus on the calculation of the potential distribution within a stress corrosion crack based on the microelectrode theory of metal corrosion.

2. Mathematical model

Consider the schematic illustration of a stress corrosion crack in Fig. 1. L is the crack length in the x-direction of the crack growth.

Based on the microelectrode theory of metal corrosion, there are many microelectrodes on the inner-surface of a stress corrosion crack. If a stress corrosion crack can be considered as an electrode which consists of n microelectrodes, an equivalent circuit of the electrode kinetics within the stress corrosion crack is considered (Fig. 2). The symbols φ_{s_i} is the galvanic potential of the electrode at position x_i; φ_{l_i} is the galvanic potential of the electrolyte at position x_i; dR_{s_i} is the metal resistance between x_i and x_{i+1}; dR_{l_i} is the solution resistance between x_i and x_{i+1}; and R_{bi} is the electrochemical reactive equivalent resistance of the electrode at position x_i.

Figure 3 shows a microcircuit from x_i to x_{i+dx} in the equivalent circuit shown in Fig. 2. The electrochemical kinetics are analysed as follows. The electrode overpotential, η, at position x within the crack is given by

$$\eta = (\varphi_s - \varphi_l)_x - (\varphi_s - \varphi_l)_e \tag{1}$$

where φ_s and φ_l are the galvanic potential of the electrode and the electrolyte at position x in the crack, respectively; $(\varphi_s - \varphi_l)_x$ is the electrode potential at position x within the crack; $(\varphi_s - \varphi_l)_e$ is the equilibrium electrode potential at the position x within the crack.

The overpotential change in the x-direction can be described as

$$d\eta = d(\varphi_s - \varphi_l)_x = (dR_{s_i} - dR_{l_i})(I_0 - I)$$
$$= \left(\rho_s \frac{dx}{tw} - \rho_l \frac{dx}{ts(x)}\right)(I_0 - I) \tag{2a}$$

where R_s and R_l are the resistances of the metal and the electrolyte, respectively; dR_s and dR_l are the resistance changes of the metal and the electrolyte, respectively; I_0 is the total polarization current passing through the equivalent circuit; I is the net polarization current from integrating 0 to x in Fig. 2; ρ_s and ρ_l are the specific resistances of the metal and the electrolyte, respectively; t is the specimen thickness; w is the specimen width; $S(x)$ is the crack width at position x.

At the position $x + dx$ in the equivalent circuit, the overpotential is given by Ohm's law

$$\eta = (R_b + r)\frac{dI}{t\,dx} \tag{3}$$

where R_b is the electrochemical reactive equivalent resistance of the electrode, r is the surface film equivalent resistance.

If $i(x)$ is the current density at position $x + dx$ in Fig. 3, it is given by Equation 3 as

$$i(x) = \frac{\eta}{R_b + r} \tag{4}$$

Since the metal resistance is very small, Equation 2 may be simplified to:

$$\frac{d\eta}{dx} = -\frac{\rho_l}{ts(x)}(I_0 - I) \tag{2b}$$

The equations above can be analysed for different conditions.

2.1. *R_b, r and ρ_l are constant, and the width between the crack tip and the mouth is equal*

Differentiating Equation 2b,

$$\frac{d^2\eta}{dx^2} = \frac{\rho_{l_0}}{tS_0}\frac{dI}{dx} \tag{5}$$

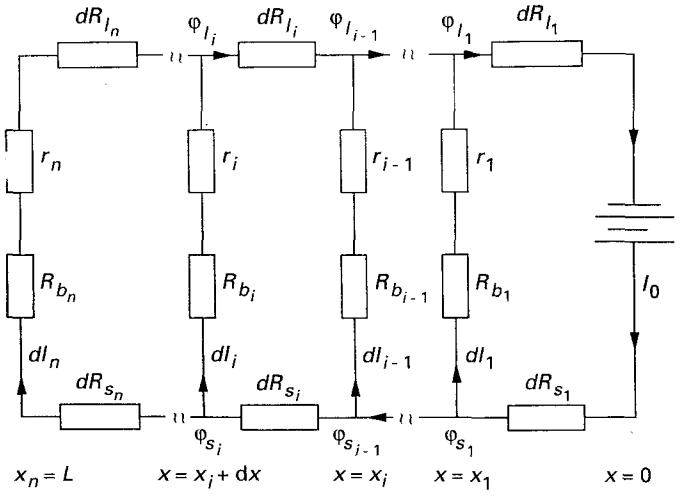

Fig. 2. An equivalent circuit of the electrochemical model within a stress corrosion crack.

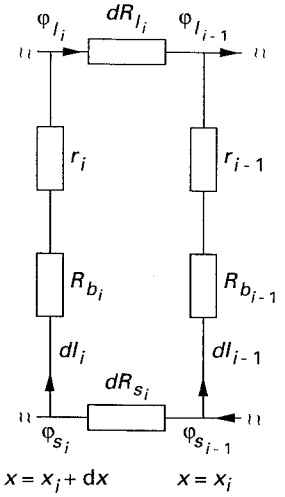

Fig. 3. A microcircuit from x to $x + dx$ in the equivalent circuit.

where ρ_{l_0} is the specific resistance of the electrolyte, and S_0 is the crack width. Both of these are constant.

Combining Equations 3 and 5 gives

$$\frac{d^2\eta}{dx^2} - \frac{\rho_{l_0}}{S_0(R_{b_0} + r_0)}\eta = 0 \tag{6}$$

The solution of Equation 6 is

$$\eta = A_1 e^{\sqrt{(b_0)}x} + A_2 e^{-\sqrt{(b_0)}x} \tag{7}$$

where $b_0 = \rho_{l_0}/S_0(R_{b_0} + r_0)$; A_1 and A_2 are integration constants. According to different boundary conditions, the Equation 7 has different forms.

2.1.1. Natural corrosion condition. The distributions of potential and current within the crack under this condition are given with respect to the boundary conditions $\eta_{x=0} = \varphi_{corr} - \varphi_e$ and $(d\eta/dx)l_{x=0} = 0$:

$$\eta = (\varphi_{corr} - \varphi_e)ch\sqrt{(b_0)}x \tag{8}$$

$$i(x) = \frac{\varphi_{corr} - \varphi_e}{R_{b_0} + r_0} ch\sqrt{(b_0)}x \tag{9}$$

where φ_{corr} is the natural corrosion potential of the electrode in the crack mouth, and φ_e is the equilibrium electrode potential in the crack mouth.

2.1.2. Applied polarization potential condition. The distributions of the potential and current within the stress corrosion crack under polarization conditions are given with respect to the boundary conditions $\eta_{x=0} = V - \varphi_e$ and $(d\eta/dx)l_{x=0} = 0$:

$$\eta = (V - \varphi_e)ch\sqrt{(b_0)}x - \frac{\rho_{l_0}I_0}{S_0\sqrt{(b_0)}} sh\sqrt{(b_0)}x \tag{10}$$

$$i(x) = \frac{1}{R_{b_0} + r_0} \times \left[(V - \varphi_e)ch\sqrt{(b_0)}x - \frac{\rho_{l_0}I_0}{S_0\sqrt{(b_0)}} sh\sqrt{(b_0)}x\right] \tag{11}$$

where V is the polarization potential.

2.2. The crack width is a linear function of x as shown in Fig. 4. R_b, r and ρ_l are constant

According to Fig. 4, the crack width can be written as

$$s(x) = s_L + (s_0 - s_L)\frac{L - x}{L} \tag{12}$$

Combining Equations 2, 3 and 12 gives

$$\frac{d^2\eta}{dx^2} - \frac{1}{s_L L/(s_0 - s_L) + L - x}\frac{d\eta}{dx} - \left(\frac{L}{s_0 - s_L}\right) \times \left(\frac{\rho_{l_0}}{R_{b_0} + r_0}\right)\left(\frac{1}{[s_L L/(s_0 - s_L)] + L - x}\right)\eta = 0 \tag{13}$$

Let

$$\frac{s_L L}{s_0 - s_L + L - x = y} \tag{14}$$

$$\left(\frac{L}{s_0 - s_L}\right)\left(\frac{\rho_{l_0}}{R_{b_0} + r_0}\right) = \tfrac{1}{4}\xi_0 \tag{15}$$

Substituting Equations 14 and 15 into Equation 13, gives

$$\frac{d^2\eta}{dy^2} + \frac{1}{y}\frac{d\eta}{dy} - \frac{\xi_0}{4y}\eta = 0 \tag{16}$$

This equation has the following solution:

$$\eta = B_1 I_0\sqrt{(\xi_0 y)} + B_2 K_0\sqrt{(\xi_0 y)} \tag{17}$$

where B_1 and B_2 are integration constants determined by the boundary conditions, and $I_0\sqrt{(\xi_0 y)}$ and $K_0\sqrt{(\xi_0 y)}$ are zero order modified Bessel functions of the first and second kinds, respectively. These can be expressed as

$$I_0\sqrt{(\xi_0 y)} = \sum_{k=0}^{\infty} \frac{1}{(K!)^2}\left(\frac{\sqrt{(\xi_0 y)}}{2}\right)^{2K} \tag{18}$$

$$K_0\sqrt{(\xi_0 y)} = -\ln\left(\frac{\sqrt{(\xi_0 y)}}{2} + \Upsilon\right) + \sum_{k=0}^{\infty} \frac{1}{(K!)^2}\sqrt{\left(\frac{(\xi_0 y)}{2}\right)^{2K}} \sum_{m=1}^{K} \frac{1}{n} \tag{19}$$

The distribution equations of the potential and the current within the stress corrosion crack with B_1 and B_2 determined by different boundary conditions are given as follows.

2.2.1. Natural corrosion condition. In natural corrosion conditions, the distribution equations of the potential and the current within the stress corrosion crack become

$$\eta = (\varphi_{corr} - \varphi_e)\sqrt{(\xi_0 y_0)}[K_1\sqrt{(\xi_0 y_0)}I_0\sqrt{(\xi_0 y)} + I_1\sqrt{(\xi_0 y_0)}K_0\sqrt{(\xi_0 y)}] \tag{20}$$

$$i(x) = \frac{(\varphi_{corr} - \varphi_e)}{R_{b_0} + r_0}\sqrt{(\xi_0 y_0)}[K_1\sqrt{(\xi_0 y_0)}I_0\sqrt{(\xi_0 y)} + I_1\sqrt{(\xi_0 y_0)}K_0\sqrt{(\xi_0 y)}] \tag{21}$$

where $I_1\sqrt{(\xi_0 y_0)}$ and $K_1\sqrt{(\xi_0 y_0)}$ are one order modified Bessel Functions of the first and second kinds. These are given by

$$I_1\sqrt{(\xi_0 y_0)} = \sum_{K=0}^{\infty} \frac{1}{K!}\frac{1}{(K+1)!}\left(\frac{\sqrt{(\xi_0 y_0)}}{2}\right)^{2K+1} \tag{22}$$

$$K_1\sqrt{(\xi_0 y_0)} = \left(\ln\frac{\sqrt{(\xi_0 y_0)}}{2} + \Upsilon\right) I_1\sqrt{(\xi_0 y_0)} - \frac{1}{2}\sum_{K=0}^{\infty}\frac{1}{K!}\frac{1}{(K+1)!}\left(\frac{\sqrt{(\xi_0 y_0)}}{2}\right)^{2K+1} \tag{23}$$

2.2.2. Applied polarization potential condition. The distribution equations of the potential and the current within the stress corrosion crack under

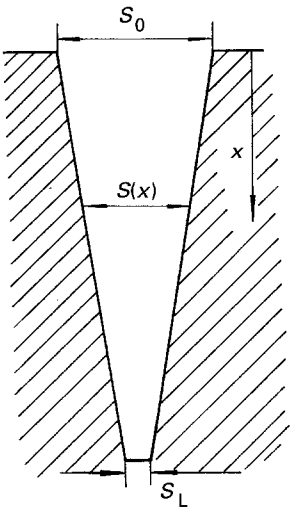

Fig. 4. A linear variation of the crack width.

Table 1. Expressions of $\xi(\eta, y)$ for different polarization conditions

Crack depth/mm	*Natural corrosion condition*	*Anodic polarization condition*	*Cathodic polarization condition*
8	$\xi(\eta,y) = 0.133\,35\left(1-\frac{x}{10}\right)^3$ $(0 \leqslant x \leqslant 8)$	$\xi(\eta,y) = 0.0304 - 4\times10^{-6}\eta_a + (0.102\,95 + 4\times10^{-6}\eta_a)\times\left(1-\frac{x}{10}\right)^3$ $(100\,\text{mV} \leqslant \eta_a \quad 0 \leqslant x \leqslant 8)$	
12	$\xi(\eta,y) = 0.089\left(1-\frac{x}{15}\right)^3$ $(0 \leqslant x \leqslant 12)$	$\xi(\eta,y) = 0.0305 - 3.5\times10^{-6}\eta_a + (0.058\,95 + 3.5\times10^{-6}\eta_a)\times\left(1-\frac{x}{15}\right)^3$ $(100\,\text{mV} \leqslant \eta_a \quad 0 \leqslant x \leqslant 12)$	$\xi(\eta,y) = 0.091 + 2\times10^{-5}\eta_c - (200+2\eta_c)\times10^{-5}\times\left(1-\frac{x}{15}\right)^3$ $(-500\,\text{mV} \leqslant \eta_c \leqslant 0 \quad 0 \leqslant x \leqslant 12)$ $\xi(\eta,y) = 0.078 + 3\times10^{-5}(600+\eta_c) + (0.011 - 3\times10^{-5}(600+\eta_c))\left(1-\frac{x}{15}\right)^3$ $(-600\,\text{mV} \geqslant \eta_c \quad 0 \leqslant x \leqslant 12)$
16	$\xi(\eta,y) = 0.0669\left(1-\frac{x}{20}\right)^3$ $(0 \leqslant x \leqslant 16)$	$\xi(\eta,y) = 0.0303 - 3\times10^{-6}\eta_a + (0.0364 + 3\times10^{-6}\eta_a)\times\left(1-\frac{x}{20}\right)^3$ $(100\,\text{mV} \leqslant \eta_a \quad 0 \leqslant x \leqslant 16)$	$\xi(\eta,y) = 0.068 + 2\times10^{-5}\eta_c - (130+2\eta_c)\times10^{-5}\times\left(1-\frac{x}{20}\right)^3$ $(-500\,\text{mV} \leqslant \eta_c \leqslant 0 \quad 0 \leqslant x \leqslant 16)$ $\xi(\eta y) = 0.0555 + 2.5\times10^{-5}(600+\eta_c) + (680 - (1500+2.5\eta_c))\times10^{-5}\left(1-\frac{x}{20}\right)^3$ $(-600\,\text{mV} \geqslant \eta_c \quad 0 \leqslant x \leqslant 16)$
20	$\xi(\eta,y) = 0.053\,35\left(1-\frac{x}{25}\right)^3$ $(0 \leqslant x \leqslant 20)$	$\xi(\eta,y) = 0.0302 - 2\times10^{-6}\eta_a + (0.023\,15 + 2\times10^{-6}\eta_a)\times\left(1-\frac{x}{25}\right)^3$ $(100\,\text{mV} \leqslant \eta_a \quad 0 \leqslant x \leqslant 20)$	$\xi(\eta,y) = 0.054 + 1\times10^{-5}\eta_c - (65+\eta_c)\times10^{-5}\left(1-\frac{x}{25}\right)^3$ $(-500\,\text{mV} \leqslant \eta_c \leqslant 0 \quad 0 \leqslant x \leqslant 20)$ $\xi(\eta,y) = 0.047 + 2\times10^{-5}(600+\eta_c) + (635 - (1200+2\eta_c))\times10^{-5}\left(1-\frac{x}{25}\right)^3$ $(-600\,\text{mV} \geqslant \eta_c \quad 0 \leqslant x \leqslant 20)$
24	$\xi(\eta,y) = 0.0445\left(1-\frac{x}{30}\right)^3$ $(0 \leqslant x \leqslant 24)$	$\xi(\eta,y) = 0.0301 - 1\times10^{-6}\eta_a + (0.0144 + 1\times10^{-6}\eta_a)\times\left(1-\frac{x}{30}\right)^3$ $(100\,\text{mV} \leqslant \eta_a \quad 0 \leqslant x \leqslant 24)$	$\xi(\eta,y) = 0.045 + 1\times10^{-5}\eta_c - (600+\eta_c)\times10^{-5}\times\left(1-\frac{x}{30}\right)^3$ $(-500\,\text{mV} \leqslant \eta_c \leqslant 0 \quad 0 \leqslant x \leqslant 24)$ $\xi(\eta,y) = 0.0385 + 1.5\times10^{-5}(600+\eta_c) + (590 - (900+1.5\eta_c))\times10^{-5}\left(1-\frac{x}{30}\right)^3$ $(-600\,\text{mV} \geqslant \eta_c \quad 0 \leqslant x \leqslant 24)$

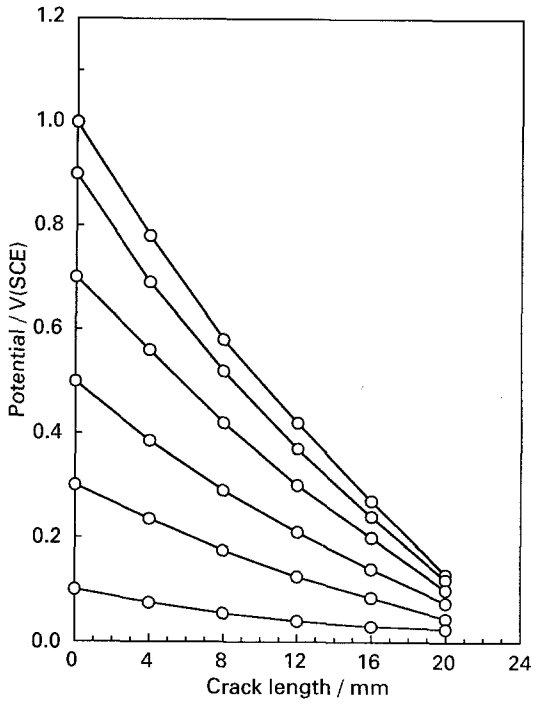

Fig. 5. Calculated potential distributions within a stress corrosion crack under anodic polarization conditions.

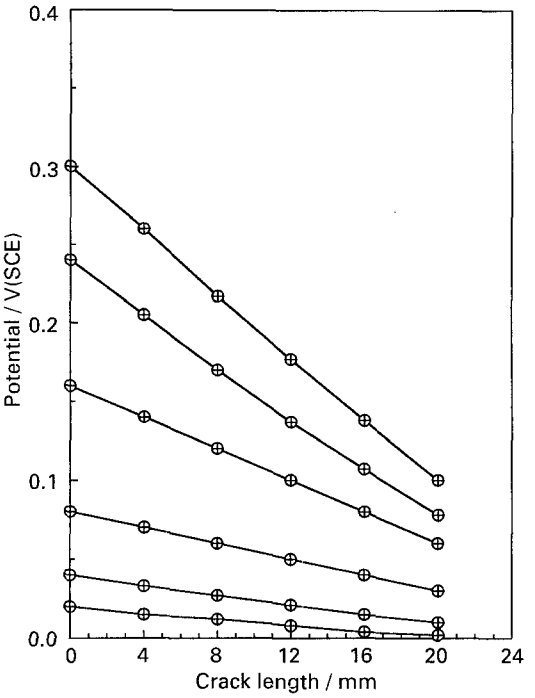

Fig. 6. Calculated potential distributions within a stress corrosion crack under natural corrosion conditions.

polarization conditions are given by

$$\eta = (V-\varphi_e)\sqrt{(\xi_0 y_0)}[K_1\sqrt{(\xi_0 y_0)}I_0\sqrt{(\xi_0 y)} + I_1\sqrt{(\xi_0 y_0)}K_0\sqrt{(\xi_0 y)}] + \left(\frac{y_0}{\xi_0}\right)^{1/2}\left(\frac{2\rho_{l_0} l_0}{S_0}\right) \times [K_0\sqrt{(\xi_0 y_0)}I_0\sqrt{(\xi_0 y)} - I_0\sqrt{(\xi_0 y_0)}K_0\sqrt{(\xi_0 y)}] \quad (24)$$

$$i(x) = \frac{(V-\varphi_e)}{R_{b_0}+r_0}\sqrt{(\xi_0 y_0)}[K_1\sqrt{(\xi_0 y_0)}I_0\sqrt{(\xi_0 y)} + I_1\sqrt{(\xi_0 y_0)}K_0\sqrt{(\xi_0 y)}] + \left(\frac{y_0}{\xi_0}\right)^{1/2}\left(\frac{2\rho_{l_0} I_0}{S_0}\right) \times \frac{[K_0\sqrt{(\xi_0 y_0)}I_0\sqrt{(\xi_0 y)} - I_0\sqrt{(\xi_0 y_0)}K_0\sqrt{(\xi_0 y)}]}{R_{b_0}+r_0} \quad (25)$$

2.3. *R_b, r and ρ_l are the function of the potential and the crack depth*

A linear variation of crack width is assumed as shown in Fig. 4. The differential equation of the potential distribution within the stress corrosion crack can be written as

$$\frac{d^2\eta}{dy^2} + \frac{1}{y}\frac{d\eta}{dy} - \frac{\xi(\eta,y)}{4y}\eta = 0 \quad (26)$$

where

$$\xi(\eta,y) = 4\frac{L}{s_0 - s_L}\left(\frac{\rho_L(\eta,y)}{R_b(\eta,t)} + r(\eta,y)\right) \quad (27)$$

3. Calculation and discussion

Theoretical calculations of the potential distribution within the stress corrosion crack in conditions of natural corrosion and applied polarization are made based on Equations 20 and 24. The $\xi(\eta,y)$ in Equations 20 and 24 vary with both potential and crack length. Expressions used in the calculation for the different conditions are shown in Table 1. In the natural corrosion condition, $\xi(\eta,y)$ depends only on the crack length. But in the anodic polarization or cathodic polarization conditions, $\xi(\eta,y)$ is a function of the polarization potential and the crack depth.

The calculated potential distributions within the crack for anodic polarization conditions are shown in Fig. 5. It is found that: (i) the crack tip potential increases slightly with increase in applied potential, and the greater the applied potential, the smaller the change in the crack tip potential; (ii) the effect of applied potential on the potential within the stress corrosion crack decreases with position from the crack mouth to tip, i.e. the nearer the crack tip, the smaller effect of the applied potential on the potential within the crack.

Figure 6 shows the calculated potential distribution within the stress corrosion crack in natural corrosion conditions. It is found that the potential within the crack is lower than that at the crack mouth.

The potential distribution within the crack for cathodic polarization is shown in Fig. 7. The potential within the crack is seen to vary greatly with increasing polarization potential.

From Figs 5 and 7, it can be seen that the longer the crack, the smaller the effect of the applied potential on

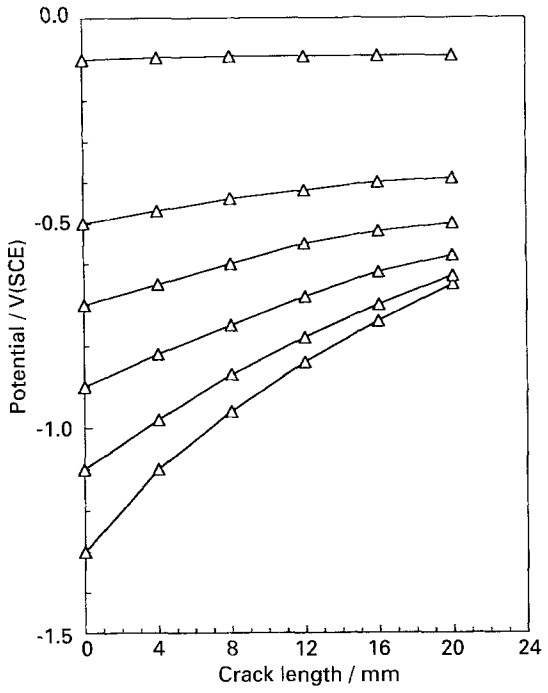

Fig. 7. Calculated potential distributions within a stress corrosion crack under cathodic polarization conditions.

the crack tip potential for both anodic and cathodic polarization conditions.

The calculated relationships between the potential of the crack tip and the crack mouth from Equation 24 are shown in Fig. 8. This shows that the crack tip potential changes slightly with applied potential for anodic polarization, but it changes greatly with applied potential for cathodic polarization.

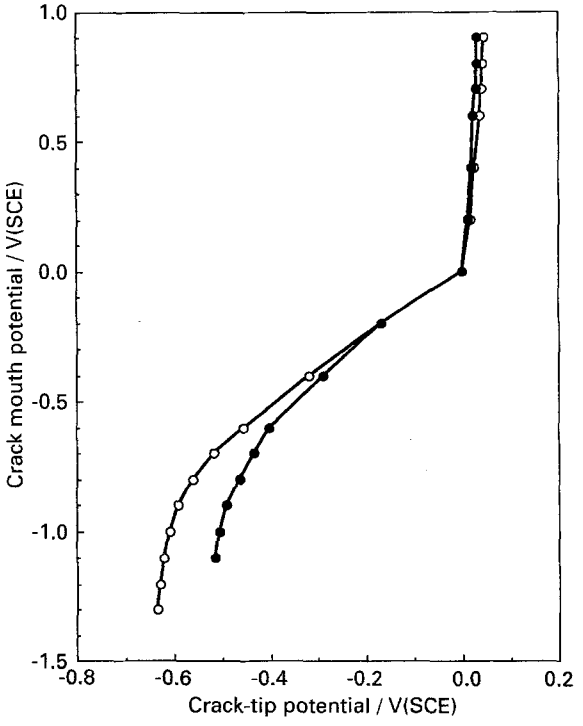

Fig. 8. Calculated relationships between crack tip potential and crack mouth. Key: (○) $x = 12$ mm, (●) $x = 16$ mm.

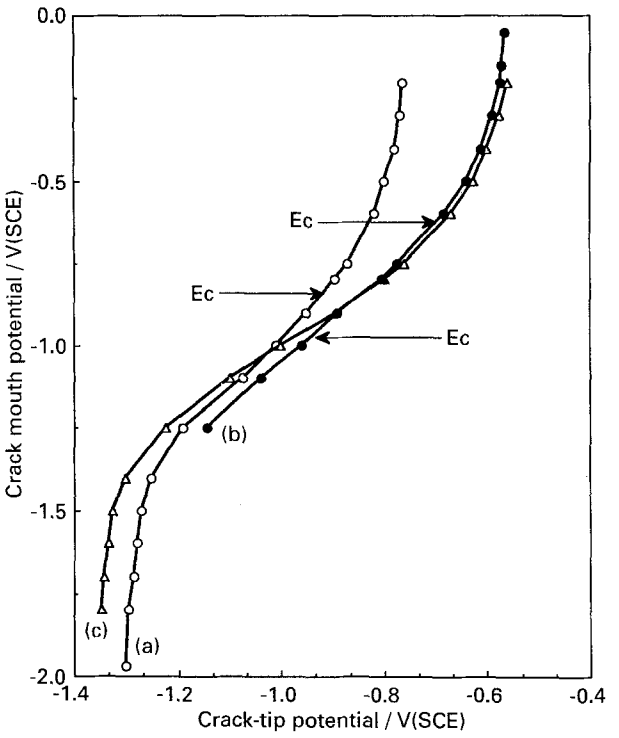

Fig. 9. Measured relationships between crack tip potential and applied polarization potential. Key: (○) Curve (a) [6]; (●) curve (b) [7]; (△) curve (c) [8].

Measured results for different systems [6–8] are reported in Fig. 9. Curve (a) is the result for aluminium alloy in 3.5% NaCl solution at room temperature. The author used an AgCl microelectrode as a reference electrode to measure directly the crack tip potential of the stress corrosion cracking specimen under polarization conditions. Curve (b) is the result for high strength steel in 3.5% NaCl solution at room temperature. The specimen was exposed to a 3.5% NaCl solution to measure directly the crack tip potential using an AgCl microelectrode as a reference electrode under polarization conditions. Curve (c) is a result of the present authors using an AgCl microelectrode as a reference electrode to measure the potential within an artificial crack made from a high strength steel sheet with a plexiglass glass. Although curves (a)–(c) were obtained from different systems, they have similar regularity.

Comparing Figs 8 and 9, the calculated results are in good agreement with previous experimental results.

4. Conclusions

The theoretical equation for potential distribution within a stress corrosion crack based on the microelectrode theory of metal corrosion is suggested as

$$\eta = (V - \varphi_e)\sqrt{(\xi_0 y_0)}[K_1\sqrt{(\xi_0 y_0)}I_0\sqrt{(\xi_0 y)} + I_1\sqrt{(\xi_0 y_0)}K_0\sqrt{(\xi_0 y)}] + \left(\frac{y_0}{\xi_0}\right)^{1/2}\left(\frac{2\rho_{l_0} l_0}{S_0}\right) \times [K_0\sqrt{(\xi_0 y_0)}I_0\sqrt{(\xi_0 y)} - I_0\sqrt{(\xi_0 y_0)}K_0\sqrt{(\xi_0 y)}]$$

The calculations show that the crack tip potential changes slightly with increasing polarization potential under anodic polarization conditions; however, it changes greatly under cathodic polarization conditions. The longer the crack, the smaller the effect of applied potential on the crack tip potential for both anodic and cathodic polarization. The theoretical calculations are in good agreement with previous experimental results.

References

[1] P. Doig and P. E. J. Flewitt, *Metal. Trans.* **9A** (1978) 357.
[2] *Idem, Proc. Roy. Soc. London* **A357** (1977) 439.
[3] *Idem*, Proceedings of the International Conference on 'Mechanism of Environment-Sensitive Cracking of Materials', University of Surrey, London: The Metals Society (1977) p. 113.
[4] P. M. Melvill, *Brit. Corros. J.* **14** (1979) 15.
[5] *Idem, ibid.* **15** (1980) 26.
[6] Z. Huang, *J. Chin. Soc. Corros. & Protect.* **4** (1984) 30.
[7] C. Xuan, *J. Iron & Steel Res.* **3** (1983) 118.
[8] Z. Huang and D. Li, *J. Chin. Soc. Corros. & Protect.* **6** (1986) 187.